ELSEVIER

Biophysical Chemistry 110 (2004) 49–58

Biophysical Chemistry

www.elsevier.com/locate/bpc

Conformation of poly(sodium ethacrylate) in solution studied by small-angle X-ray scattering

Yoshio Muroga[a,*], Shozo Iida[b], Shigeru Shimizu[c], Hiroki Ikake[c], Kimio Kurita[c]

[a] *Department of Applied Chemistry, Graduate School of Engineering, Nagoya University, Furo-cho, Chikusa-ku, Nagoya 464-8603, Japan*
[b] *Department of Physics, Graduate School of Science, Nagoya University, Furo-cho, Chikusa-ku, Nagoya 464-8603, Japan*
[c] *Department of Materials and Applied Chemistry, College of Science and Technology, Nihon University, 1-8-14 Kandasurugdai, Chiyoda-ku, Tokyo 101-8308, Japan*

Received 24 November 2003; received in revised form 5 January 2004; accepted 5 January 2004
Available online 27 April 2004

Abstract

The pH-induced conformational transition of poly(sodium ethacrylate) PNaEA in aqueous solution, which occurs between a compact form at low charge-density and an extended coil at high charge-density, was studied by small-angle X-ray scattering and the structure at an each conformational state was analyzed and compared with the corresponding one of poly(sodium methacrylate) PNaMA. The conformational transition for PNaEA induced a remarkable change in the scattering data plotted in the form of the Kratky plot. By comparing the scattering data with theoretical scattering functions, it was clarified that the structures of the compact form and the extended coil are well mimicked by a swollen gel having a network structure and by a wormlike chain, respectively. Although such a structure of the extended coil of PNaEA is similar to the corresponding one of PNaMA, the structure of the compact form of PNaEA is different from the corresponding one of PNaMA, which is still represented by a wormlike chain in a Θ medium.

Keywords: Poly(ethacrylic acid); Conformational transition; Small angle X-ray scattering; Wormlike chain; Dendrimer; Poly(methacrylic acid)

1. Introduction

Poly(methacrylic acid) PMA and poly(ethacrylic acid) PEA have both ionizable group and hydrophobic group and the sodium salts, poly(sodium methacrylate) PNaMA and poly(sodium ethacrylate) PNaEA, show similar pH-induced conformational transitions in aqueous solution between a compact form at low charge-density and an extended coil at high charge-density, as is well known [1–5]. However, it is supposed that the structures of the compact forms and the extended coils of PNaMA and PNaEA should be different from each other, because α-substituent in these polyelectrolytes, methyl group and ethyl group, respectively, have different hydrophobic natures in aqueous solution, although the backbone-structure of the chain and the ionizable group, carboxylic group are common in these polymers.

* Corresponding author. Tel.: +81-52-789-4822; fax: +81-52-789-4822.
E-mail address: ymuroga@apchem.nagoya-u.ac.jp (Y. Muroga).

0301-4622/$ - see front matter © 2004 Elsevier B.V. All rights reserved.
doi:10.1016/j.bpc.2004.01.002

The potentiometric-titration studies [3–5] have shown that the standard free-energy change ΔG° (ca. 2500 J/mol) of PNaEA in the conformational transition from an uncharged compact form to an uncharged extended coil is several times larger than that of PNaMA (ca. 700 J/mol). Our recent small-angle X-ray scattering (SAXS) study [6] has shown that the compact form and the extended form of PNaMA are represented by a wormlike chain in a Θ medium and with an excluded-volume effect, respectively. However, a difference between the conformations of PNaMA and PNaEA has not been fully clarified yet.

The present paper is devoted to analyze the structure at an each conformational state of PNaEA in added-salt aqueous solution by SAXS and compare the structure with corresponding one of PNaMA.

2. Materials and methods

Ethacrylic acid was prepared from diethyl ethylmalonate according to the method by Böhme and Teltz [7]. It was polymerized in a 5.0% aqueous solution of the monomer using a mixture of $K_2S_2O_8$ (1 w/w% of the monomer) and $NaHSO_3$ (0.25% w/w) as an initiator. When the solution was kept at 50–60 °C under the nitrogen atmosphere, it gradually turned turbid and a milky suspension was obtained after approximately 12 h. The reaction mixture was kept at the temperature for further few days and then purified by dialysis against distilled water with membrane tubing (Spectra/Por, MWCO:3500; Spectrum Medical Industries, Inc.). The ^{1}H-NMR spectrum of PNaEA having the degree of ionization i=0.9 thus prepared is shown in Fig. 1, which was recorded in D_2O at 60 °C on Varian UNITY INOVA 500 (500 MHz). A hump at ~1 ppm is assigned to methyl protons in the side chains and another hump at ~2 ppm to methylene protons in the side and main chains. The area under the former and the latter humps are in the ratio ca. 3:4, as expected. The apparent molecular weight ($1–2\times10^5$) and the distribution index (Mw/Mn ~ 1.6) were evaluated on the basis of poly(ethylene oxide) by gel permeation chromatography on JASCO GPC 8020 (column GMHHR) using *N*,*N*,-dimethylformamide DMF as elution solvent at 40 °C.

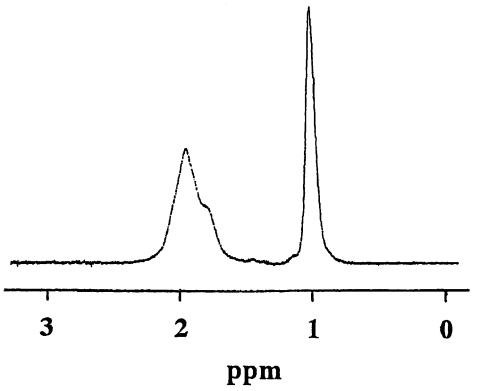

Fig. 1. ^{1}H-NMR spectrum of PNaEA having i=0.9 in D_2O at 60 °C.

The potentiometric titration was carried out to see the pH-induced conformational transition of PNaEA, using Corning M255 pH meter at 20±1.0 °C under bubbling of Ar gas over the solution in order to avoid contamination of the solution by atmospheric CO_2. PEA was substantially insoluble in water and formed a suspension. However, when NaOH was added to the suspension, a clear solution was obtained and a sharp titration-end-point was reached with further addition of NaOH. Accordingly, back titration was done with the clear solution of PNaEA.

The relationship between pK_a and the degree of ionization i at added salt (NaCl) concentration C_s=0.1 M is given in Fig. 2 for PEA (×) at the concentration of ionizable group of 0.00167 N, together with the existing data [8] of PMA (△) and poly(acrylic acid) PAA (○), where pK_a is defined by pH+log{(1−i)/i}. It is clearly shown that the data of PMA and PEA have a hump in a lower i range, whereas those of PAA has no hump, indicating that the pH-induced conformational transition occurs in PMA and PEA, and the hump of PEA is much larger than that of PMA. Taking into account that PNaEA in aqueous solution assumes a compact form at i < ~0.2 and an extended coil at i > ~0.6, i of PNaEA for SAXS experiments was adjusted to be 0.2 and 0.8 in 0.1 M NaCl aqueous solution and 0.2, 0.3, 0.4 and 0.8 in 0.033 M NaCl aqueous solution. PEA (i=0) in DMF solution was employed as a reference sample. The polymer concentrations C_p were adjusted to be 0.5–1.12 g/dl for all samples.

The SAXS experiments were carried out using synchrotron orbital radiation as an X-ray source set

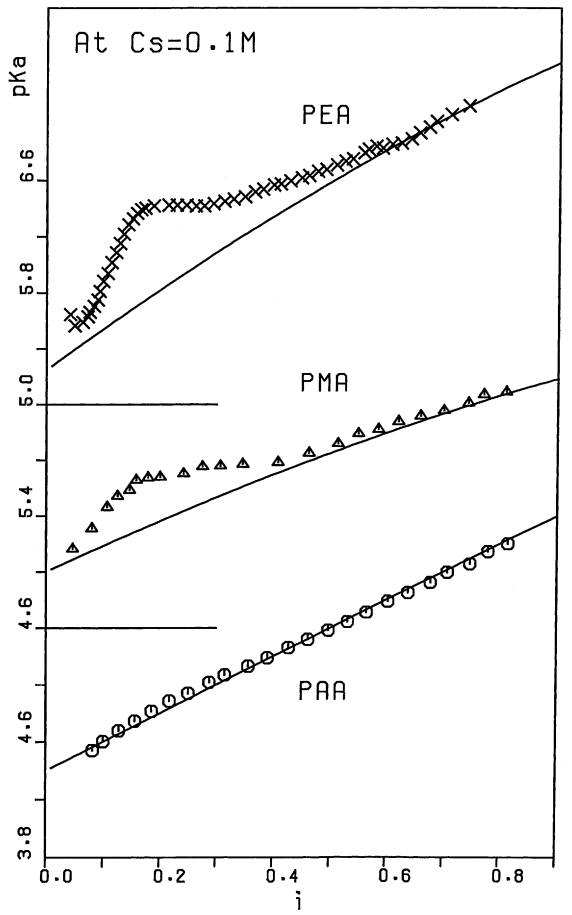

Fig. 2. The relationship between pK_a and i at C_s=0.1 N for poly(acrylic acid) (○) [8], poly(methacrylic acid) (△) [8] and poly(ethacrylic acid) (×).

up in the Photon Factory of the High Energy Accelerator Organization at Tsukuba, Ibaragi, Japan. The wavelength of the X-ray λ was 1.488 Å and the distance between the sample and the detector was 95 cm. The scattered intensity was detected by a position-sensitive proportional counter (PSPC) with 512 channels over a scattering vector q from 0.02 to 0.25 $Å^{-1}$, where q is defined by $(4\pi/\lambda)\sin(\theta/2)$, and θ is a scattering angle. The details of the instrumentation and the procedure are described elsewhere [9]. Effects of slit-length and slit-width on the scattering curves were neglected, because the size of the X-ray beam at the sample position was small enough compared with the camera length. Scattered intensities were registered on a relative scale, not on an absolute scale and so they were allowed to be multiplied by a constant factor for comparison with theoretical curves.

3. Results and discussion

Fig. 3 shows the Guinier plot, $\ln(I)$ vs. q^2 for PNaEA in NaCl aqueous solution with (A) i=0.2: C_s=0.033 N and C_p=0.56 g/dl (○), C_s=0.1 N and C_p=0.50 g/dl (△); (B) i=0.3: C_s=0.033 N and C_p=0.67 g/dl (+); (C) i=0.4: C_s=0.033 N and C_p=0.83 g/dl (×); (D) i=0.8: C_s=0.033 N and C_p=0.63 g/dl (◇), C_s=0.1 N and C_p=0.50 g/dl (↑), C_s=0.1 N and C_p=0.80 g/dl (⊠) and for PEA (i=0) in DMF solution (E) C_p=0.63 g/dl (symbol Z) and C_p=1.12 g/dl (symbol Y), where I is observed scattering intensity. The scattering data for samples having different C_p and C_s in the samples (A), (D) and (E) were reduced to those at a reference state by multiplying them with a constant factor and the data sets thus reduced were shifted by a suitable magnitude along the ordinate for easy discrimination of each data set. Since the reduced data almost coincide with each other, as shown in the figure, an effect of interparticle interferences on I would be small under the present experimental condition and intermolecular associations between different particles would be negligible.

The mean-squared radius of gyration $\langle R_g^2\rangle$ of a particle is estimated with the Guinier plot from the slope of a straight line drawn through the scattering data in a range of q^2 below q^{*2} (=$1/\langle R_g^2\rangle$). Scattering data form straight lines below q^{*2}, indicated by an arrow above an each curve, for all samples except the samples (E), where the linear region appears around q^{*2}. The root mean-squared radius of gyration $\langle R_g^2\rangle^{1/2}$ thus estimated are listed in Table 1. It is seen that $\langle R_g^2\rangle^{1/2}$ for PNaEA in aqueous solution increases gradually from 23±5 Å at i=0.2 to 37±5 Å at i=0.8. However, they are smaller than $\langle R_g^2\rangle^{1/2}$ for PEA in DMF 46±5 Å, showing that attractive hydrophobic interactions between α-ethyl groups would effectively work in aqueous solutions over a wide range of i and suppress the expansion of PNaEA in aqueous solution.

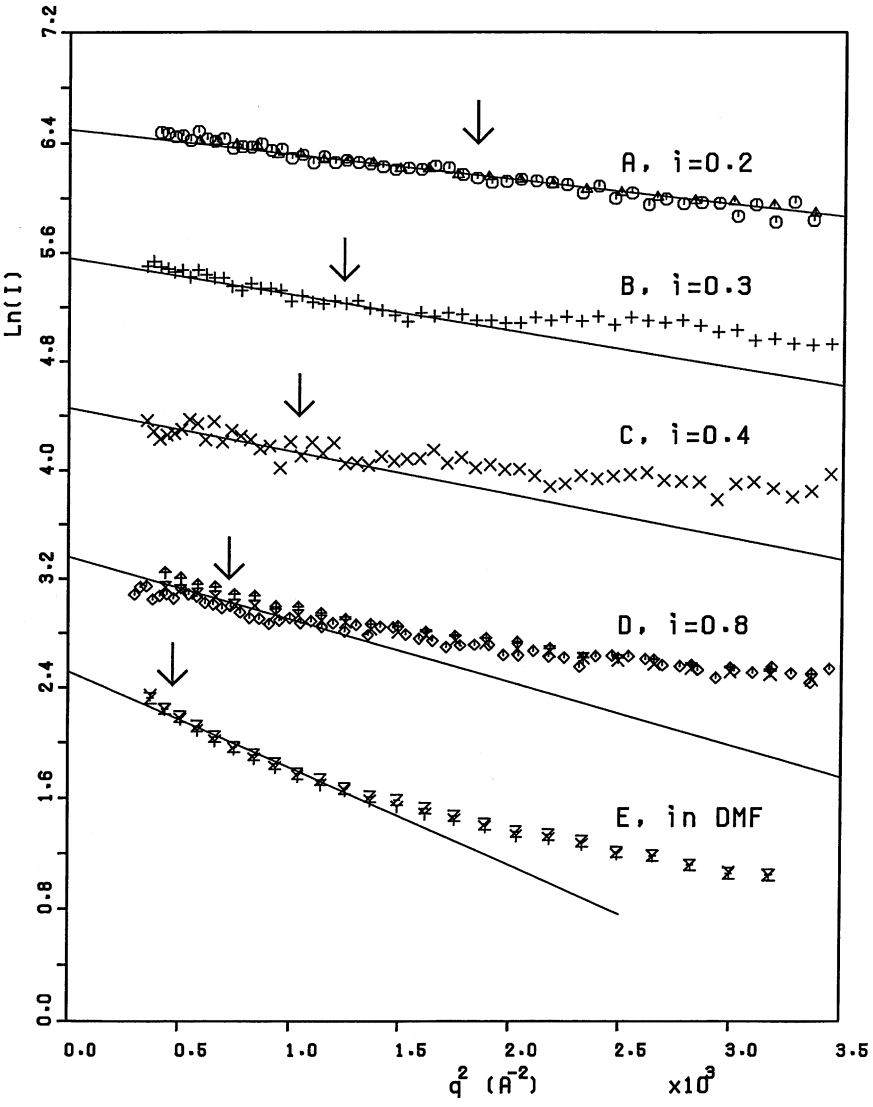

Fig. 3. The Guinier plot, ln(I) vs. q^2 for PNaEA in NaCl aqueous solution with (A) i=0.2: C_s=0.033 N and C_p=0.56 g/dl (○), C_s=0.1 N and C_p=0.50 g/dl (△); (B) i=0.3: C_s=0.033 N and C_p=0.67 g/dl (+); (C) i=0.4: C_s=0.033 N and C_p=0.83 g/dl (×); (D) i=0.8: C_s=0.033 N and C_p=0.63 C_p=0.63 g/dl (◇), C_s=0.1 N and C_p=0.50 g/dl (↑), C_s=0.1 N and C_p=0.80 g/dl (⊠); and for PEA (i=0) in DMF solution (E): C_p=0.63 g/dl (symbol Z) and C_p=1.12 g/dl (symbol Y). Solid straight lines are drawn through the scattering data in a range of q^2 less than $1/\langle R_g^2\rangle$. An arrow above an each curve shows q^2 equal to $1/\langle R_g^2\rangle$.

A critical concentration C_p* in g/dl, where two isolated polymer chains begin to overlap with each other, can be evaluated by [10]:

$$C_p^* = \frac{100M}{(4/3)\pi R^3 N_A} \quad (1)$$

where M, R and N_A are the molecular weight, the radius of polymer chain and Avogadro's number. Substituting the molecular weight and $R=(5/3)^{1/2}\langle R_g^2\rangle^{1/2}$, where $\langle R_g^2\rangle^{1/2}$ are listed in Table 1, into Eq. (1), C_p* for the most expanded form (PEA in DMF solution) is roughly estimated to be ~60 g/dl, which is much larger than C_p employed for the samples, ca.

Table 1
Observed data and molecular parameters obtained from analysis of SAXS curves

Data set	Solvent	C_p (g/dl)	i	$\langle R_g^2\rangle^{1/2}$ (Å)	b (Å)	n	N	K	ξ (Å)	$\langle R_g^2\rangle^{1/2}_{calc}$ (Å)
A	0.033 N NaCl	0.56	0.2	23±5	5	7	5	0	–	23
A	0.1 N NaCl	0.5	0.2	23±5	5	7	5	0	–	23
B	0.033 N NaCl	0.67	0.3	28±5	5	32	3	0.3	20	32
					N_T=450, N_b=2, f=2					

Data set	Solvent	C_p (g/dl)	i	$\langle R_{cs}^2\rangle^{1/2}$ (Å)	$\langle R_g^2\rangle^{1/2}$ (Å)	P_l (Å)	ε	K	ξ (Å)	$\langle R_g^2\rangle^{1/2}_{calc}$ (Å)
C	0.033 N NaCl	0.83	0.4	31±5	–	–	–	–	–	–
D	0.033 N NaCl	0.63	0.8	37±5	3.3±0.3	3.5	0.015	0.4	20	42
D	0.1 N NaCl	0.5	0.8	37±5	3.3±0.3	3.5	0.015	0.4	20	42
D	0.1 N NaCl	0.8	0.8	37±5	3.3±0.3	3.5	0.015	0.4	20	42
E	DMF	0.63	0	46±5	3.3±0.3	5.5	0.015	0.2	10	44
E	DMF	1.12	0	46±5	3.3±0.3	5.5	0.015	0.2	10	44
							L=980 (Å)			

1 g/dl. Thus the degree of overlap of polymer chains is conceived to be significantly low for all samples.

As was reviewed by Porod [11], scattering intensity $I_{rod}(q)$ of a rod having a length l and the mean-squared radius of a cross-section of the rod $\langle R_{cs}^2\rangle$ is given by the product of the axial factor $I_{thin}(q)$ and the cross-sectional factor $I_{cs}(q)$:

$$I_{rod}(q) \propto I_{thin}(q) \cdot I_{cs}(q) \tag{2}$$

$$I_{thin}(q) \propto \frac{l\pi}{q} \tag{3}$$

$$I_{cs}(q) \propto \exp\left\{-\frac{1}{2}\langle R_{cs}^2\rangle \cdot q^2\right\} \tag{4}$$

Therefore, if the local conformation of a flexible chain were approximated by a rod, the scattering data plotted in the form of $\ln(I{\cdot}q)$ vs. q^2 would form a straight line in a range of q^2:

$$\frac{1}{\langle R_g^2\rangle} < q^2 < \frac{1}{\langle R_{cs}^2\rangle} \tag{5}$$

and $\langle R_{cs}^2\rangle$ would be estimated from the slope of the straight line with Eqs. (2)–(4). Fig. 4 shows the plot for PNaEA in 0.1 N NaCl aqueous solution, where the symbols have the same meanings as those in Fig. 3 and the data sets were shifted by a suitable magnitude along the ordinate. For PNaEA with i=0.8 in aqueous solution (D) and for PEA in DMF solution (E), the scattering data form a straight line in a q^2 range of Eq. (5) and the slopes give $\langle R_{cs}^2\rangle^{1/2}$=3.2–3.3±0.3 Å, comparable with ca. 3.7 Å expected for the trans-zigzag conformation, where an arrow above an each curve indicates $q^2=1/\langle R_{cs}^2\rangle$. For the compact form at i=0.2 (A), however, any straight lines, temporarily drawn through the scattering data, give an extraordinary large $\langle R_{cs}^2\rangle^{1/2}$, indicating that the local structure for the compact form cannot be regarded as a rod. $\langle R_{cs}^2\rangle^{1/2}$ of PNaMA has been shown to be 3.0–4.2±0.3 Å over an entire range of i [6].

In Fig. 5a, the scattering data of PNaEA are plotted in the form of the Kratky plot $I{\cdot}q^2$ vs. q, where the symbols have the same meanings as those in Fig. 3. In Fig. 5b are replotted the existing data [6] of PNaMA in 0.1 N NaF aqueous solution and PMA in MeOH, (A): PNaMA, i=0 and C_p=1.3 g/dl (○); (B): PNaMA, i=0.15 and C_p=0.89 g/dl (△); (C): PNaMA, i=0.3 and C_p=1.1 g/dl (+); (D): PNaMA, i=1.0 and C_p=1.1 g/dl (×); (E): PMA, i=0 and C_p=1.10 g/dl (◇). While the profiles for PNaMA in aqueous solution are little varied with i, those of PNaEA are significantly affected with i. The i dependence of the conformations for PNaMA and PNaEA would be different from each other.

The scattering function $P(q)$ for a wormlike chain with and without excluded volume effect are given by Sharp and Bloomfield [12] in terms of contour length L of a polymer chain, persistence length P_l and excluded parameter ε, where ε is defined by the ratio of the mean-square end-to-end distance $\langle r^2\rangle$ of a polymer containing t links to its value $\langle r^2\rangle_o$ when there is no excluded volume effect:

$$\frac{\langle r^2\rangle}{\langle r^2\rangle_o} = t^{\varepsilon} \tag{6}$$

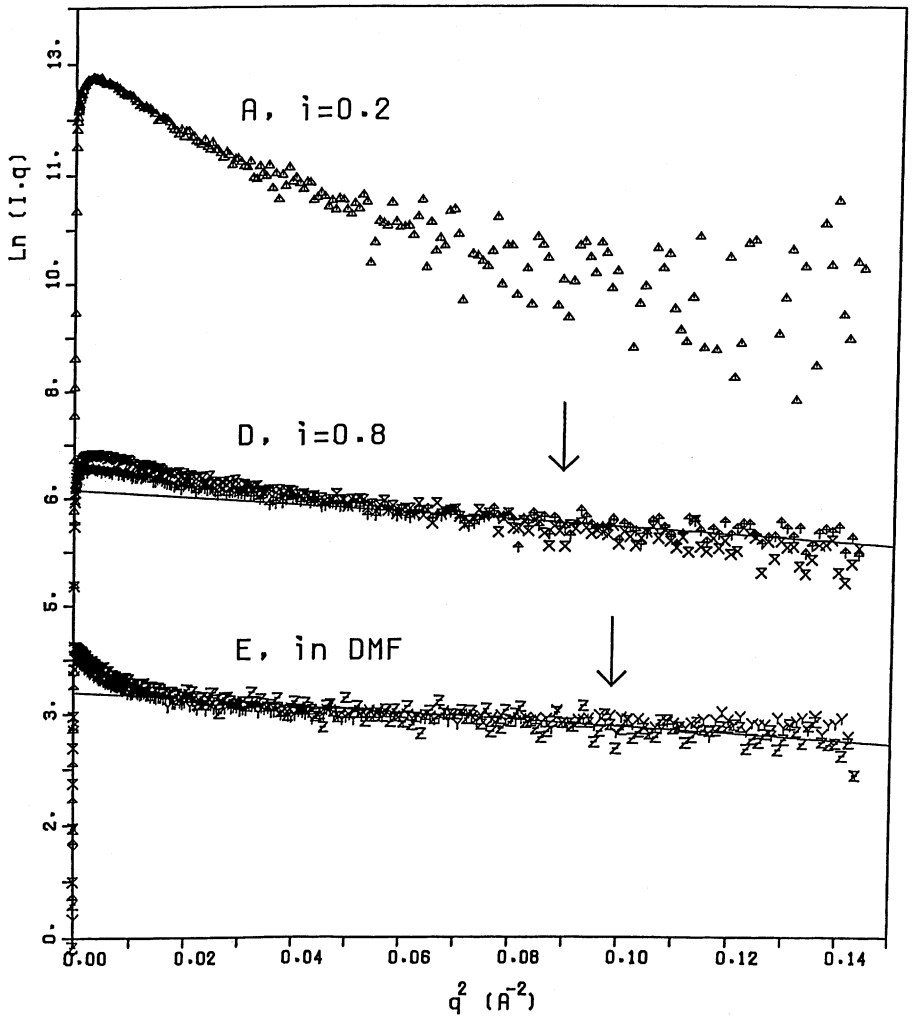

Fig. 4. The plot of $\ln(I{\cdot}q)$ vs. q^2 for PNaEA in 0.1 *N* NaCl aqueous solution with (A): i=0.2 and C_p=0.50 g/dl (△); (D): i=0.8 and C_p=0.50 g/dl (↑); i=0.8 and C_p=0.80 g/dl (⊠) and for PEA (i=0) in DMF solution (E) with C_p=0.63 g/dl (symbol Z) and C_p=1.12 g/dl (symbol Y). Solid straight lines are drawn through the scattering data in a range of q^2 of Eq. (4). An arrow above an each curve shows q^2 equal to $1/\langle R_{cs}^2\rangle$.

The mean-squared radius of gyration $\langle R_g^2\rangle_o$ for a wormlike chain with no excluded volume effect was given by Benoit and Doty [13]. $\langle R_g^2\rangle$ for a wormlike chain with excluded volume effect is evaluated from $\langle R_g^2\rangle_o$, assuming a following relation:

$$\frac{\left\langle R_g^2\right\rangle}{\left\langle R_g^2\right\rangle_o} = t^{\varepsilon} \tag{7}$$

The degree of overlap of polymer chains in solution is suggested to be significantly low, but one cannot completely exclude a possibility of slight intermolecular-interferences between different molecules. Thus, the scattering curves were analyzed with a scattering factor $Q(q)$ taking into account both intramolecular- and intermolecular-interferences between charges or segments, where $Q(q)$ is the product of a scattering factor $I_{\text{particle}}(q)$ for a single particle and an interference factor $S(q)$ between different particles. That is,

$$Q(q) \propto I_{\text{particle}}(q) \cdot S(q) \tag{8}$$

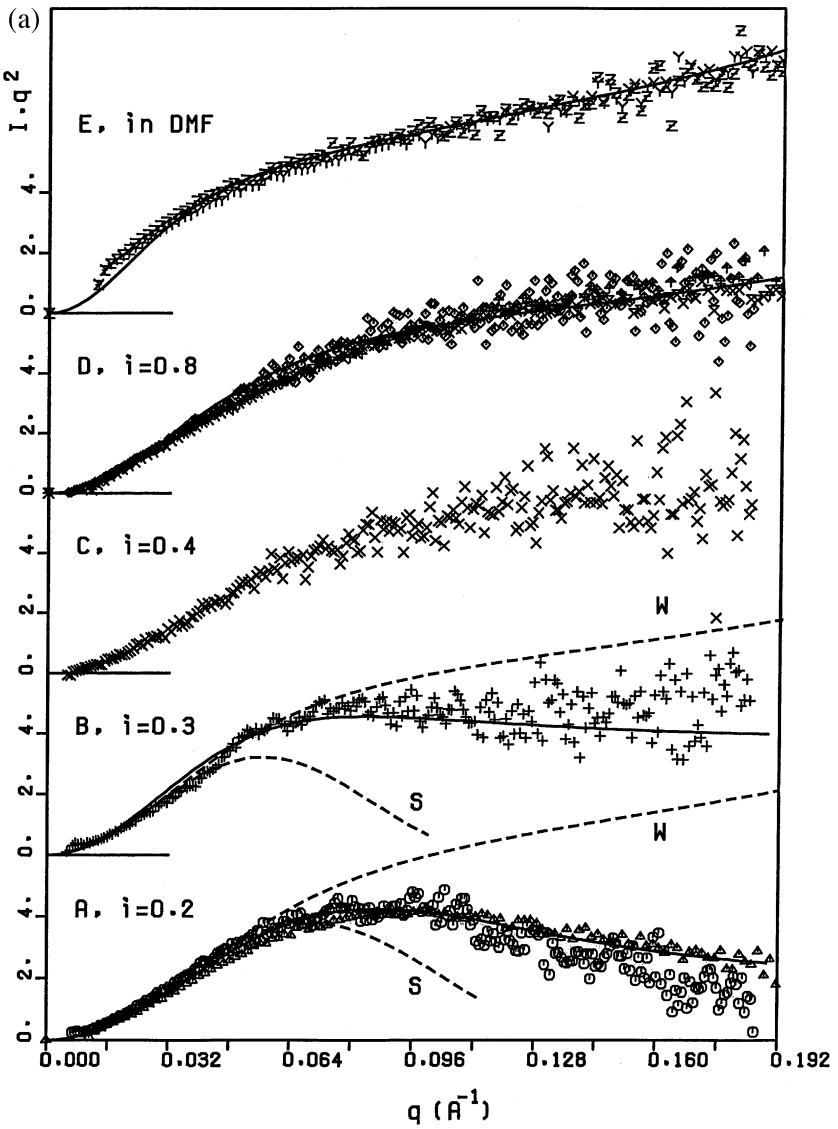

Fig. 5. (a) The Kratky plot $I{\cdot}q^2$ vs. q for PNaEA. Symbols have the same meaning as those in Fig. 3. Solid curves in the data sets A and B and in the data sets D and E are theoretical curves for a dendrimer and for a wormlike chain, respectively, where values for the molecular parameters employed are listed in Table 1. Dotted curves with symbol w and with symbol s in the data sets A and B are theoretical curves for a wormlike chain and for a hard-sphere, respectively. (b) The Kratky plot $I{\cdot}q^2$ vs. q for PNaMA in 0.1 N NaF aqueous solution and PMA in MeOH, (A): PNaMA, i=0 and C_p=1.3 g/dl (○); (B): PNaMA, i=0.15 and C_p=0.89 g/dl (△); (C): PNaMA, i=0.3 and C_p=1.1 g/dl (+); (D): PNaMA, i=1.0 and C_p=1.1 g/dl (×); (E): PMA, i=0 and C_p=1.10 g/dl (◇). Solid curves are theoretical curves for a wormlike chain.

where

$$S(q) \propto \frac{1}{\{1 + K \cdot \exp(-\xi^2 q^2)\}} \qquad (9)$$

K is a constant, which reflects the degree of intermolecular interactions and is approximately given by $2A_2M_wC_p$, where A_2 is a second virial coefficient and ξ denotes correlation length of intermolecular interaction, which represents a range of interaction

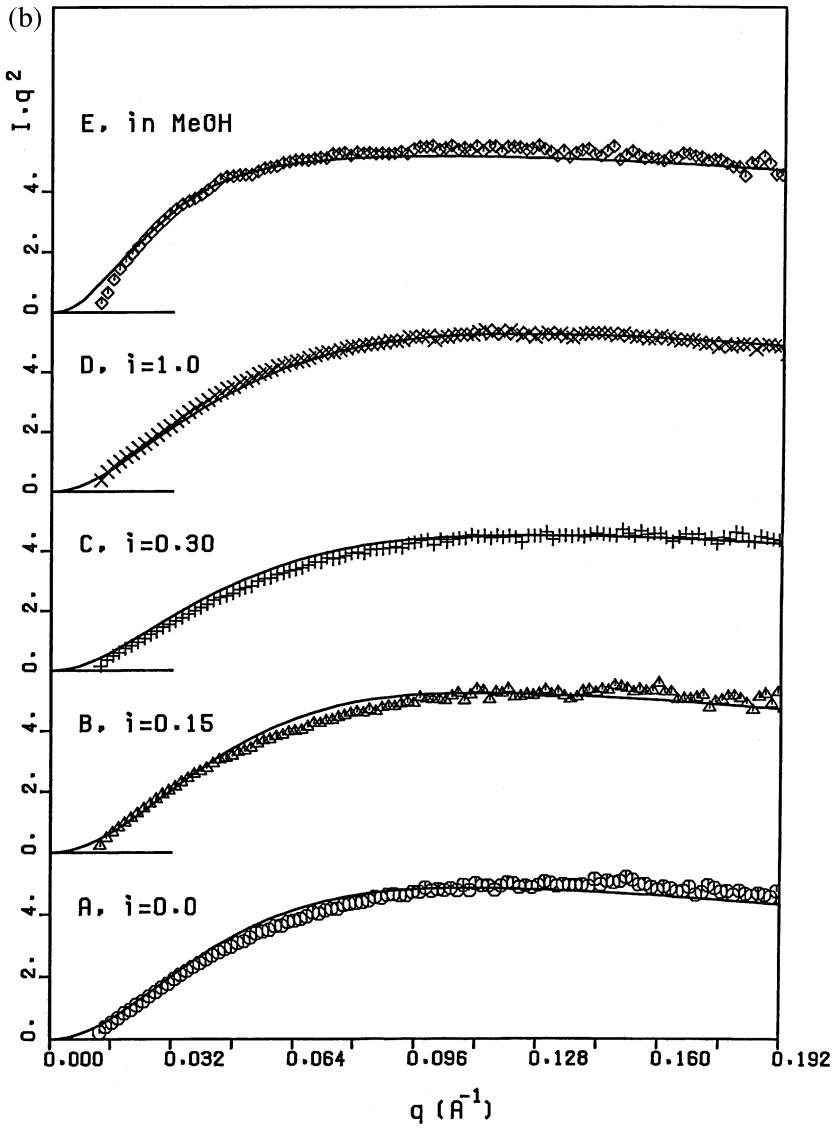

Fig. 5 (*continued*).

[14]. Therefore, using $P(q)$ for the wormlike chain having no cross-section, $Q(q)$ for the wormlike chain having a finite cross-section is given by:

$$Q(q) \propto P(q) \cdot \exp\left\{-\frac{1}{2}\langle R_{cs}^2\rangle q^2\right\} \cdot S(q) \qquad (10)$$

Expecting that both extended coils of PEA in DMF solution and PNaEA at i=0.8 in aqueous solution would behave as wormlike chains, the scattering data (E) and (D) in Fig. 5a, respectively, and their $\langle R_g^2\rangle^{1/2}$ are compared with the corresponding theoretical ones for a wormlike chain, which are computed with Eqs. (7) and (10). The scattering data (C) at i=0.4 seems to show an intermediate behavior between the extended coil and the compact form and has not been analyzed further. Solid curves at data (D) and (E) in Fig. 5a are theoretical curves for a wormlike chain computed

with (D): P_l=3.5 Å, K=0.4, ξ=20 Å and (E): P_l=5.5 Å, K=0.2, ξ=10 Å, where L=980 Å, $\langle R_{cs}^2\rangle^{1/2}$=3.3 Å and ε=0.015 are common in both samples. The agreement between the observed data and the theoretical curves is satisfactory and $\langle R_g^2\rangle_{calc}^{1/2}$ computed for the two wormlike chains, 42 Å (D) and 44 Å (E), are comparable with the observed ones, 37±5 Å (D) and 46±5 Å (E) (Table 1). Accordingly, a contribution of $S(q)$ to $Q(q)$ could be negligible over a whole q range.

As shown in Fig. 5b, the scattering data for PNaMA in aqueous solution and for PMA in MeOH are also well reproduced by a theoretical curve (a solid curve) for a wormlike chain, computed with (A): P_l=4 Å, ε=0, K=0.5, ξ=20 Å, $\langle R_{cs}^2\rangle^{1/2}$=3.9 Å; (B): P_l=4 Å, ε=0, K=0.6, ξ=20 Å, $\langle R_{cs}^2\rangle^{1/2}$=3.8 Å; (C): P_l=4 Å, ε=0.06, K=0.6, ξ=20 Å, $\langle R_{cs}^2\rangle^{1/2}$=3.8 Å; (D): P_l=4 Å, ε=0.08, K=0.6, ξ=20 Å, $\langle R_{cs}^2\rangle^{1/2}$=4.1 Å; (E): P_l=6 Å, ε=0, K=0, $\langle R_{cs}^2\rangle^{1/2}$=3.9 Å, where L=1090 Å is common in all samples [6]. That is, the conformations of PNaEA at i=0.8 and also PNaMA over an entire range of i are satisfactorily mimicked by a wormlike chain having P_l of 5.0–5.5 Å and 4 Å, respectively. To be noted here, the compact forms of PMA at i=0 and PNaMA at i=0.15 are still represented by a wormlike chain in a Θ medium [6].

However, the scattering data of PNaEA at i=0.2 (A) and 0.3 (B) in Fig. 5a were not reproduced by either theoretical curve of wormlike chain (dotted curves with symbol w) or hard sphere (dotted curves with symbol s): With increasing q, the theoretical curve of a wormlike chain departs upward from the observed data, whereas the theoretical curve of a hard sphere departs downward from it, where molecular parameters employed in the computations were adjusted by try-and-error so that the scattering data in a low q range, at least, and $\langle R_g^2\rangle^{1/2}$ in Table 1 could be well reproduced with the models. This result seems to suggest that the segment-densities in the compact forms of PNaEA at i=0.2 and 0.3 would be higher than that in a wormlike chain and lower than that in a hard sphere.

The requirement for the segment-density in the compact form of PNaEA might be satisfied by a swollen gel having a network structure, which consists of several branches composed of random coils. Considering that α-ethyl groups of PNaEA would have more hydrophobic natures in aqueous solution than α-methyl groups of PNaMA, it is highly probable that such a network structure would be constructed through the intramolecular associations between the α-ethyl groups. From these considerations, $P(q)$ of a gel consisting of regular multi branches, so-called dendrimer, was applied for analyzing the conformations of PNaEA at i=0.2 and 0.3. $P(q)$ for a dendrimer were derived by Burchard et al. [15] and Hammouda [16]. Here, the one developed by Hammouda was employed, which leave the functionality as an arbitrary parameter. The dendrimer is regularly formed of N_b branches. Each branch is formed of N generations of monomeric blocks. The number of blocks is multiplied by a factor f in going from one generation to the next. Each block is composed of n links having length b forming Gaussian chains. At the data (A) and (B) in Fig. 5a, the solid curves are theoretical curves for dendrimers, computed with N=5, n=7 and K=0 and N=3, n=32, K=0.3 and ξ=20 Å, respectively, where the total number of links N_T=450, N_b=2, f=2 and b=5 Å are common in the both models (Table 1). The agreement between the observed data and the theoretical curves is satisfactory and $\langle R_g^2\rangle_{calc}^{1/2}$, 23 Å and 32 Å, computed for the models are comparable with the observed ones, 23±5 Å and 28±5 Å, respectively. Moreover, the contour length (L) derived from N_T=450, 1125 Å, is reasonably close to one assigned to samples (D) and (E), 980 Å.

As a consequence, the compact form of PNaEA at low charge density is better mimicked by a swollen gel having a network structure, rather than by a wormlike chain or a hard sphere. Such a conformation for the compact form of PNaEA is different from that of the compact form of PNaMA in acidic aqueous solution, which is still represented by a wormlike chain in a Θ medium [6]. Since the extended coils of PNaEA and PNaMA are equally mimicked by wormlike chains having comparable P_l, the difference between ΔG° (ca. 2500 J/mol) of PNaEA and that of PNaMA (ca. 700 J/mol) would arise from the difference between the structures of their compact forms.

4. Conclusion

The pH-induced conformational transition of poly(sodium ethacrylate) PNaEA in aqueous solution, which occurs between a compact form at low charge-density and an extended coil at high charge-density,

was studied by small-angle X-ray scattering and the structure at an each conformational state was analyzed and compared with the corresponding one of poly (sodium methacrylate) PNaMA. The structures of the compact form and the extended coil of PNaEA are well mimicked by a swollen gel having a network structure and by a wormlike chain, respectively. Although such a structure of the extended coil of PNaEA is similar to the corresponding one of PNaMA, the structure of the compact form of PNaEA is different from the corresponding one of PNaMA, which is still represented by a wormlike chain in a Θ medium.

References

[1] J.C. Leyte, M. Mandel, Potentiometric behavior of polymethacrylic acid, J. Polym. Sci. Part A1 2 (1964) 1879–1891.
[2] V. Crescenzi, F. Quadrifoglio, F. Delben, Calorimetric investigation of poly(methacrylic acid) and poly(acrylic acid) in aqueous solution, J. Polym. Sci. Part A2 10 (1972) 357–368.
[3] F. Fichtner, H. Schönert, Kooperative Zuständsanderung von Polyäthylacrylsaure in wäßriger Lösung, Colloid Polym. Sci. 255 (1977) 230–232.
[4] D.E. Joyce, T. Kurucsev, Hydrogen ion equilibria in poly(methacrylic acid) and poly(ethacrylic acid) solutions, Polymer 22 (1981) 415–417.
[5] S. Sugai, K. Nitta, N. Ohno, H. Nakano, Conformational studies on poly(ethacrylic acid) in aqueous salts by potentiometric, viscometric, optical and ^{1}H-NMR measurements, Colloid Polym. Sci. 261 (1983) 159–165.
[6] Y. Muroga, T. Yoshida, S. Kawaguchi, Conformation of poly(methacrylic acid) in acidic aqueous solution studied by small angle X-ray scattring, Biophys. Chem. 81 (1999) 45–57.
[7] H. Böhme, H.P. Teltz, Über Darstellung und Umwandlungsprodukte von Oxymethyl-alkyl-malonestern, Arch. Pharm. 288 (1955) 343–346.
[8] M. Nagasawa, T. Murase, K. Kondo, Potentiometric titration of stereoregular polyelectrolytes, J. Phys. Chem. 69 (1965) 4005–4012.
[9] T. Ueki, Y. Hiragi, Y. Izumi, H. Tagawa, M. Kataoka, Y. Muroga, T. Matsushita, Y. Amemiya, Photon Factory Activity Report (1982/1983) VI70–VI71.
[10] P.G. de Gennes, Scaling Concept in Polymer Physics, Cornell University Press, Ithaca, New York, 1979, pp. 76–77.
[11] G. Porod, in: O. Glatter, O. Kratky (Eds.), Small Angle X-ray Scattering, Academic Press, New York, 1982, pp. 32–35.
[12] P. Sharp, V.A. Bloomfield, Light Scattering from Wormlike Chains with Excluded Volume Effects, Biopolymers 6 (1968) 1201–1211, with a correction in C.W. Schmid, F.P. Rinehart, J.E. Hearst, Biopolymers 10 (1971) 833.
[13] H. Benoit, P. Doty, Light scattering from non-gaussian chains, J. Phys. Chem. 57 (1953) 958–963.
[14] T. Coviello, H. Maeda, Y. Yuguchi, H. Urakawa, K. Kajiwara, M. Dentini, V. Crescenzi, Conformational characteristics of oxidized scleroglucan, Macromolecules 31 (1998) 1602–1607.
[15] W. Burchard, K. Kajiwara, D. Nerger, Static and dynamic scattering behavior of regularly branched chains: a model of soft-sphere microgels, J. Polym. Sci. Part B 20 (1982) 157–171.
[16] B. Hammouda, Structure factor for starburst dendrimers, J. Polym. Sci. Part B 30 (1992) 1387–1390.